MODELING AND SCALING LAWS FOR LARGE FIRES

Howard R. Baum
Building and Fire Research Laboratory
National Institute of Standards and Technology
Gaithersburg, MD 20899 USA

ABSTRACT

Mathematical models of the convective transport induced by large fires are presented. The models are chosen to illustrate the role of scaling laws in the mathematical development and computer implementation of simulations. The basic equations governing large fire dynamics are presented in a form suitable for these studies. The role of vorticity and heat release is emphasized in this formulation. Two different fire scenarios are examined; each with a unique analysis aimed at the phenomena of interest. First, a "kinematic" approach to fire plume dynamics is used to relate vorticity and heat release distributions obtained from plume correlations to fire induced winds. The utility of this approach is illustrated by appeal both to experiments on individual laboratory plumes and simulations of mass fires. The interaction of fire plumes with atmospheric winds is illustrated by a smoke dispersion model that couples a simplified description of the stratified atmosphere with a CFD based simulation of the large scale fire induced motions. Simulations of crude oil fire plumes compared with large scale experiments are shown to demonstrate the use of this model. A brief discussion of additional factors involved in the analysis of large fires is outlined.

INTRODUCTION

Large fires can be characterized by the nature of their interaction with the local environment. The environment as defined here consists of a description of the geometry and burning characteristics of the fuel bed, the properties of the ambient atmosphere, and the geography of the natural terrain and buildings in the spatial domain of interest. The physical processes that control these interactions determine the various length scales that define the dynamics of a given fire scenario. One of the most obvious features of any fire is the enormous range of active length scales, ranging from the sub-millimeter thickness of an individual flame to the kilometer sized convective transport scales in large smoke plumes. Since it is not feasible to develop approximate models that include such a wide range of phenomena, a plausible way to trucate this large dynamic range is required.

An isolated fire in a quiescent laboratory environment can be described in terms of a single macroscopic plume length scale $D^\star$, defined in more detail below. All combustion reactions, diffusion, and local turbulent mixing occur on scales small compared with $D^\star$. Thus, the fire is described in terms of an overall heat release rate which determines $D^\star$. This can be accomplished by making use of empirical correlations which have the consequences of the smaller scale dynamics built into them. Large fires then, possess additional length scales that are comparable to or larger than the plume length scale. These scales arise either because of the nature of the fire scenario, as in mass fires, or because the physical processes that must be considered occur at atmospheric dynamics scales. Examples of each of these will be given below.

The paper is organized as follows: The "low Mach number combustion" equations governing the dynamics of fire plumes are presented in the next section. The fluid mechanical properties of these equations are explored, with particular emphasis on the mechanisms of vorticity creation and volumetric expansion. The remainder of the paper consists of two sections that describe mathematical models of different fire scenarios. Each of these models is chosen because the role of scaling laws is of critical importance in both formulating the models and in obtaining solutions. The first is based on a "kinematic" approach, using the fact that the sources of vorticity and expansion in fire plumes can be readily inferred from standard plume correlations. The fire induced flow is then directly related to the strength of these sources. The results show that the concept of entrainment is readily explained in terms of buoyancy induced vorticity. Moreover, this simple model can be used to predict some complex flow phenomena observed in large fires.

The second model introduces a simplified description of the interaction of a buoyant plume with a stratified atmospheric wind. The Boussinesq approximation together with the assumption that the component of the fluid velocity in the direction of the atmospheric wind is

undisturbed by the presence of the fire permits the development of a high resolution plume dynamics computer code. The code has been used to calculate the three-dimensional dispersion of combustion products in the atmosphere based on the fundamental equations with minimal computer resources.

These models can be thought of as representing two limiting scenarios of interest in the study of large fires. The kinematic model is an inherently "near field" description of an idealized urban mass fire. The dimensions of the fire bed are much larger than any individual fire. The collective behavior of the totality of fires is the prime object of interest in this context. The wind blown plume model is a "far field description". The dynamics of the fire bed is completely lost in this analysis. Although both are idealizations of a much more complicated reality, the results outlined below indicate that even these simplified analyses capture a wide variety of observed phenomena.

FUNDAMENTALS

The starting point is the equations of motion for a compressible flow in the low Mach number approximation. However, the equations as originally developed [Rehm and Baum, 1978] must be modified to allow for an ambient pressure $P_0(z)$, temperature $T_0(z)$ and density $\rho_0(z)$ that vary with height z in the atmosphere in the absence of the fire. Their equations assume that the fire induced pressure is a small perturbation about the time dependent spatial average of the pressure in an enclosure. For the present application, the fire induced pressure $\tilde{p}$ is a small perturbation about $P_0(z)$. The ambient density and temperature are related to $P_0(z)$ by the equation of state and the assumption of hydrostatic balance in the ambient atmosphere. The equations expressing the conservation of mass, momentum, and energy then take the form:

$$\frac{D\rho}{Dt} + \rho \nabla \cdot \vec{u} = 0 \tag{1}$$

$$\rho \left(\frac{\partial \vec{u}}{\partial t} - \vec{u} \times \vec{\omega} + \nabla \left(\frac{1}{2} u^2 \right) \right) + \nabla \tilde{p} - (\rho - \rho_0)\, \vec{g} = \nabla \cdot \tau \tag{2}$$

$$\rho\, C_p \frac{DT}{Dt} - w \frac{dP_0}{dz} = -\nabla \cdot \vec{q} + Q_c \tag{3}$$

Here, ρ is the density, $\vec{u}$ the velocity, T the temperature, and $\tilde{p}$ the fire induced pressure in the gas. The unresolved momentum flux and viscous stress tensors are lumped together and denoted by τ. The quantity $\vec{\omega}$ is the fluid vorticity. The vertical component of the velocity is denoted by w in equation (3) and the hydrostatic relation between P_0 and ρ_0 has been used in equation (2). The specific heat is denoted by C_p. Similarly, the unresolved advected energy flux, the conduction heat flux, and the radiant energy flux are denoted by $\vec{q}$, while the chemical heat release per unit volume is Q_c.

The energy and momentum equations can be thought of as advancing the time evolution of T and $\vec{u}$ respectively. However the pressure perturbation does not obey an explicit time evolution equation. Instead, it is the solution of an elliptic equation determined by the divergence of the velocity field. The instantaneous response of the pressure field implied by the above equations is a consequence of the low Mach number assumption. In reality, pressure changes are carried through the atmosphere at the speed of sound. However, the sound speed is assumed to be so much higher than the local ambient winds or fire induced flows that the transit time for the sound wave can be ignored.

The equations presented above also require recipes for τ, $\vec{q}$, and the heat release from the fire. In principle, there is no difficulty writing down the well known expressions leading to the Navier-Stokes equations and the associated energy and species conservation equations. Using these expressions, there are no unresolved fluxes or stresses. If it were possible to solve the resulting equations for the problems of interest no further discussion would be needed. However, the range of dynamically active length and time scales in almost any fire scenario is much too large to be amenable to computation. Thus, approximate forms of these equations have to be employed if any results are to be obtained. The approximate equations inevitably contain assumptions about the nature and importance of the unresolved stresses and fluxes. Before considering such models, however, it is useful to extract some basic information from the most general form of the equations.

First consider the decomposition of the velocity field into its irrotational and solenoidal components. The mass and energy conservation equations together with the equation of state can be combined to yield:

$$\nabla \cdot \vec{w} = \frac{\gamma - 1}{\gamma p_\infty} \left(P_0(z)/p_\infty \right)^{-\left(\frac{\gamma-1}{\gamma}\right)} \left(-\nabla \cdot \vec{q} + Q_c \right) \tag{4}$$

$$\vec{w} = \left(P_0(z)/p_\infty \right)^{\frac{1}{\gamma}}\, \vec{u} \tag{5}$$

Here, p_∞ is a reference pressure in the ambient atmosphere far from the fire, and γ is the specific heat ratio. Equation (4) determines the divergence of the velocity field (or more precisely a "pseudo-velocity" $\vec{w}$) in terms of the combustion heat release rate and the fluxes of sensible and radiant energy.

Just as equation (4) describes the sources of the irrotational component of the velocity, the source of the

solenoidal field is the fluid vorticity $\vec{\omega}$. The evolution of the vorticity field can be related to the plume dynamics using Kelvins Theorem. Let Γ be the circulation about any closed circuit moving with the fluid. Then, [Goldstein, 1960]:

$$\frac{D\Gamma}{Dt} = \oint \vec{a} \cdot \vec{dr} \tag{6}$$

Here, $\vec{a}$ is the local acceleration of the fluid and the integral is around the closed circuit. Using equation (2):

$$\frac{D\Gamma}{Dt} = \oint \frac{1}{\rho} \left(-\nabla\tilde{p} + (\rho - \rho_0)\,\vec{g} + \nabla \cdot \tau\right) \cdot \vec{dr} \tag{7}$$

Γ is directly related to the the vorticity by Stokes Theorem:

$$\Gamma = \oint \vec{u} \cdot \vec{dr} = \int_S \vec{\omega} \cdot \vec{n}\, dS \tag{8}$$

The unit vector $\vec{n}$ is normal to the surface S bounded by the closed circuit used to define the circulation. Thus, equation (7) is an integral relation between the rate of vorticity creation and the forces on the fluid.

The above results can be exploited by explicitly decomposing the velocity field as follows:

$$\vec{u} = \nabla\phi + \vec{v} \tag{9}$$

Then, ϕ and $\vec{v}$ satisfy scalar and vector Poisson equations respectively. This is particularly clear if the stratification of the ambient atmosphere can be ignored. The equations then become:

$$\nabla^2\phi = \frac{\gamma - 1}{\gamma p_\infty} \left(-\nabla \cdot \vec{q} + Q_c\right) \tag{10}$$

$$\nabla \times \vec{v} = \vec{\omega} \qquad \nabla \cdot \vec{v} = 0 \tag{11}$$

Equations (10) and (11) demonstrate explicitly that the heat flux and heat release are the sources of the potential field and that the vorticity is the source of the solenoidal field. Moreover, equation (7) shows that in general, there are three sources of vorticity. The first term on the right hand side of this equation corresponds to the non-buoyant baroclinic vorticity generation caused by the misalignment of pressure and density gradients. Outside the fire plume it vanishes, and away from the active combustion zone this term is small. However, where most of the heat release takes place, this is a significant contributor to the vorticity [Mell et al., 1996]. The second term is the contribution of the buoyancy. It also vanishes outside the plume, but is pervasive everywhere in the plume. Because of this, it is the dominant source of the solenoidal component of the velocity field almost everywhere. The last term in equation (7) represents the effects of viscosity on vorticity creation. For almost any fire of interest, this mechanism operates at such small scales that its effects are unimportant.

The sources of the potential flow also require a distinction between large and small scale phenomena. The heat flux vector $\vec{q}$ can be decomposed into conduction and radiative components as follows:

$$\vec{q} = -k\,\nabla T + \vec{q}_R \tag{12}$$

The thermal conductivity $k(T)$ is small enough to ensure that the conduction flux is highly localized in the fire plume. The radiative flux $\vec{q}_R$, on the other hand is significant at the largest scales. Thus, if the velocity potential is decomposed in an analogous way, a large scale expansion field Φ can be defined as:

$$\phi = \frac{\gamma - 1}{\gamma p_\infty} \int_{T_\infty}^{T} k(T)\, dT + \Phi \tag{13}$$

$$\nabla^2\Phi = \frac{\gamma - 1}{\gamma p_\infty} \left(-\nabla \cdot \vec{q}_R + Q_c\right) \tag{14}$$

The temperature T_∞ is a reference temperature in the ambient atmosphere. Note that the conduction induced velocity is a highly localized flow directed *up* the temperature gradient, while the large scale potential field is the solution of a Poisson equation with an essentially positive right hand side. This is true even if the combustion energy release is contained in a large number of individual flames, each of which is much smaller than any macroscopic plume length scale.

FIRE INDUCED FLOWS

The entrainment of air into a fire plume is a neccesary condition for the fire to be sustained. However, there is no precise definition of this concept, and measurement of the "entrainment rate" has proved both difficult and controversial. The problem arises because the typical approach to determining the increase of mass in an isolated fire plume with height above the fire rests on measuring or inferring an inflow velocity at the edge of the plume. However, unlike the temperature field, the velocity does not undergo any sharp transition at the edge of the plume. Indeed, the flow quantity most like the temperature is the vorticity. Moreover, if the flow quantity to be determined is chosen to be the fire induced flow field rather than the "entrainment" then both the measurement and the modeling problem become tractable.

The starting point is the decomposition of the velocity field as represented by equations (11) and (14). Note that the right hand sides of these equations are non-vanishing only in the fire plume. Moreover, they are linear in the relations between both the solenoidal velocity and the

vorticity and the potential field and the heat release rate. Thus, if time averaged experimental data describing the structure of the vorticity and heat release fields inside the plume are available, then the time averaged velocity fields both inside and outside the plume can be determined. Similarly, if time resolved data is available, the corresponding velocities can be calculated. This observation is the basis for a "kinematic" approach to fire induced flows [Baum and McCaffrey, 1988].

First consider an isolated laboratory scale fire. The time averaged plume is axially symmetric, and the net integrated radiative flux emitted from the fire is assumed to be a fraction χ of the combustion heat release rate Q_c. Defining (r, z) as radial and vertical cylindrical coordinates measured from the center of the fire, the corresponding velocity components u_r and u_z can be expressed in terms of $\Phi(r, z)$ and a vector potential $\Psi(r, z)$ as follows:

$$u_r = \frac{\partial \Phi}{\partial r} - \frac{1}{r}\frac{\partial \Psi}{\partial z} \qquad u_z = \frac{\partial \Phi}{\partial z} + \frac{1}{r}\frac{\partial \Psi}{\partial r} \tag{15}$$

Similarly, the vorticity vector reduces to an azimuthal component $\omega_\phi(r, z)$. Now let Q_O be the total combustion heat release rate generated by the fire. Then, it is possible to define a natural plume length scale $D^\star$ as:

$$D^\star = \left(\frac{Q_O}{\rho_\infty C_p T_\infty \sqrt{g}} \right)^{2/5} \tag{16}$$

The independent variables can now be made nondimensional by introducing $(r, z) = D^\star(r^\star, z^\star)$. The dependent variables are then scaled in the form:

$$(u_r, u_z) = (gD^\star)^{1/2} \left\{ u^\star(r^\star, z^\star),\, v^\star(r^\star, z^\star) \right\} \tag{17}$$

$$(\Phi, \Psi) = D^\star (gD^\star)^{1/2} \left\{ \Phi^\star(r^\star, z^\star),\, \Psi^\star(r^\star, z^\star) \right\} \tag{18}$$

Finally the vorticity and heat release rate which act as the sources of the vector and scalar potentials are written in the form:

$$\omega_\phi = (g/D^\star)^{1/2}\, \omega^\star \qquad Q_c = [Q_O/(D^\star)^3]\, Q^\star \tag{19}$$

This choice of dimensionless variables is *not* arbitrary. The plume correlations developed by McCaffrey [McCaffrey, 1983] can be compactly expressed in this form [Baum and McCaffrey, 1988]. Moreover, if the temperature is made dimensionless with respect to T_∞ and the fire induced pressure $\tilde{p}$ is normalized with respect to $\rho_\infty g D^\star$, then all the explicitly resolved terms in the dimensionless form of the fundamental conservation equations (1), (2), and (3) depend only on the fraction of the combustion energy release emitted as radiation χ_r.

Finally the vector and scalar potentials satisfy the following equations, which exhibit the same parametric dependence:

$$\frac{\partial^2 \Psi^\star}{\partial z^{\star\,2}} + \frac{\partial^2 \Psi^\star}{\partial r^{\star\,2}} - \frac{1}{r^\star}\frac{\partial \Psi^\star}{\partial r^\star} = r^\star \omega^\star(r^\star, z^\star) \tag{20}$$

$$\frac{\partial^2 \Phi^\star}{\partial z^{\star\,2}} + \frac{1}{r^\star}\frac{\partial}{\partial r^\star}\left(r^\star \frac{\partial \Phi^\star}{\partial r^\star} \right) = (1-\chi_r) Q^\star(r^\star, z^\star) \tag{21}$$

Equations (20) and (21) must be supplemented by boundary conditions at the ground $z^\star = 0$ and far from the fire. Since there can be no flow through the ground:

$$\Psi^\star(r^\star, 0) = \frac{\partial \Phi^\star}{\partial z^\star}(r^\star, 0) = 0 \tag{22}$$

The far field boundary conditions are much more interesting. Since the heat release region is bounded in space, the potential field far from the fire corresponds to the point source solution.

$$\Phi^\star = \frac{1-\chi_r}{2\pi \left(r^{\star\,2} + z^{\star\,2} \right)^{1/2}} \tag{23}$$

The asymptotic solenoidal velocity must be that associated with a point source plume. Since the velocity field decays proportional to $(z)^{-1/3}$ in the plume, the vorticity and stream function must take the following form:

$$\Psi^\star = \left(r^{\star\,2} + z^{\star\,2} \right)^{5/3} F(\theta) \tag{24}$$

$$\omega^\star = \left(r^{\star\,2} + z^{\star\,2} \right)^{-4/3} \Omega(\theta) \tag{25}$$

Here, θ is the polar angle in a spherical polar coordinates measured from the plume centerline. The plume structure function F vanishes at $\theta = 0$ and $\theta = \pi/2$, and satisfies the equation

$$\frac{d^2 F}{d\mu^2} + \frac{10}{9\,(1-\mu^2)} F = \Omega(\mu) \qquad \mu = \cos(\theta) \tag{26}$$

The structure of the vorticity function $\Omega(\mu)$ is determined from the assumed Gaussian form of the vertical velocity profile in the plume, with the width obtained from McCaffreys correlation. The results can be expressed in terms of a spherical radial component of the velocity field $V_\rho^\star$ and polar angle component $V_\theta^\star$ which take the form:

$$V_\rho^\star = \left(r^{\star\,2} + z^{\star\,2} \right)^{-1/3} V_\rho(\theta) \tag{27}$$

$$V_\theta^\star = \left(r^{\star\,2} + z^{\star\,2} \right)^{-1/3} V_\theta(\theta) \tag{28}$$

The functions V_ρ and V_θ are plotted in Fig. 1. Note that negative values of V_θ near the plume centerline $\theta = 0$

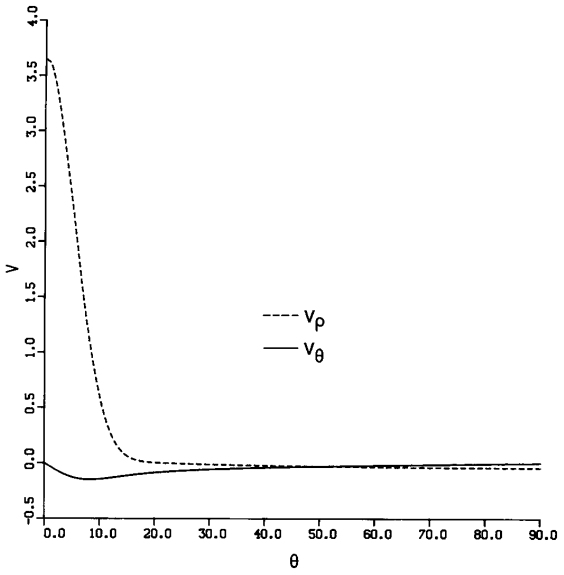

FIGURE 1: ANGULAR DEPENDENCE OF NORMALIZED RADIAL (V_ρ) AND TANGENTIAL (V_θ) VELOCITIES FOR POINT SOURCE PLUME. [Baum and McCaffrey, 1988]

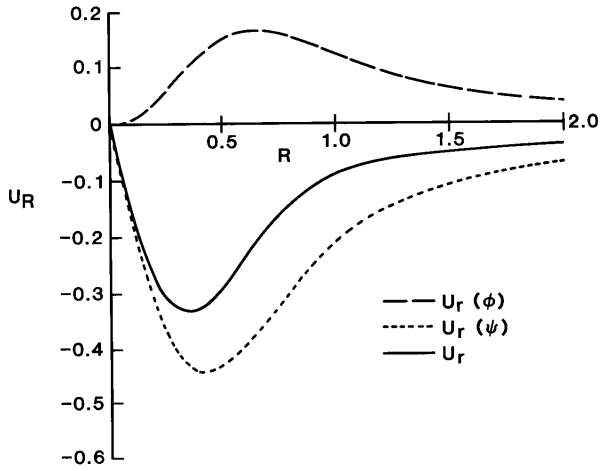

FIGURE 2: CALCULATED GROUND LEVEL RADIAL VELOCITY SHOWING EXPANSION (DASHED) AND VORTICITY INDUCED (DOTTED) CONTRIBUTION TO FLOW. [Baum and McCaffrey, 1988]

and V_ρ near the ground plane $\theta = \pi/2$ correspond to inflows into the plume which are balanced by the vertical outflow through the plume carried by V_ρ near $\theta = 0$. The flow pattern outside a point source plume was studied by Taylor [Taylor, 1958] who replaced the entire plume by a line sink. His result is equivalent to that obtained here away from the plume, but becomes singular as the plume is approached.

Using the above results as boundary conditions, equations (20) and (21) can be solved in a cylindrical domain for $\Psi^\star$ and $\Phi^\star$ using fast direct elliptic equation solvers. The right hand sides of the equations are again determined from McCaffreys correlation. Details can be found in [Baum and McCaffrey, 1988]. Fig. 2 shows the ground level radial velocity, together with the component terms. Note that the solenoidal velocity is responsible for the entrainment, while the expansion flow is actually directed outward. The expansion flow is quite significant for distances from the plume comparable to the flame height ($z^\star = 1.3$ in the present units). However, the vorticity induced flow dominates everywhere else. Moreover, the buoyancy induced component of the vorticity, which is all that survives in the far field, is by far the most important source of the vorticity.

Since the computations described above are easy to perform (the discretized elliptic equations can be solved in less than a second on a twenty thousand point grid using any current generation workstation), this model can be used to calculate the flows induced by mass fires. Almost any such fire is actually a collection of discrete fires, due to either the discrete nature of the "fuel" (individual buildings, say) or because the oxygen supply to an individual fuel parcel is consumed by adjacent fires. If attention is focused on flows at or near ground level, then the plumes associated with each fire will be distinct. Since equations (21) and (20) are linear and the vorticity fields associated with each plume are separated, then the flows induced by each fire can be added vectorially. The combined asymptotic and numerical solutions for $\Phi^\star$ and $\Psi^\star$ then constitute a "computational element" that can be scaled appropriately for any size fire with a given radiative fraction. Using this technique it is not difficult to simulate the near ground flows induced by hundreds to thousands of individual fires. Such fires were in fact the motivation for this work.

The model has been tested experimentally against large controlled burns by Quintiere and his collaborators [Quintiere, 1990], [Quintiere, 1993]. These field experiments, conducted in Canada in 1989, included wind tower measurements at five separate locations of velocities induced by fires whose ultimate strength reached several GW. Infrared photographs were used to discretize the fire into over 40 individual fires whose strength was estimated from separate analyses of the vegetation in the

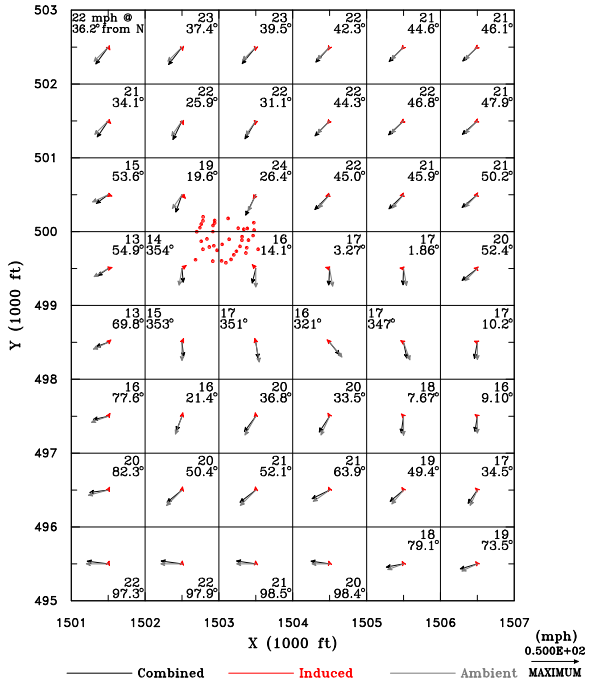

FIGURE 3: HORIZONTAL INDUCED WINDS 20 M ABOVE GROUND PLANE SHOWING 38 FIRES BURNING AT 11:45 AM. [Trelles and Pagni, 1997]

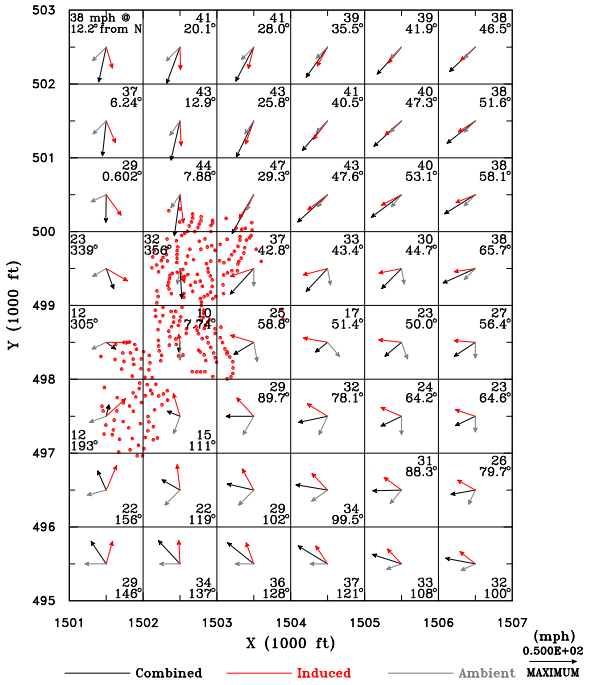

FIGURE 4: HORIZONTAL INDUCED WINDS 20 M ABOVE GROUND PLANE SHOWING 259 FIRES BURNING AT 12:00 PM. [Trelles and Pagni, 1997]

logged fields that constituted the fuel Despite the fact that the terrain consisted of low rolling hills, and numerous uncertainties in the fuel characterization, the agreement between the calculated and measured horizontal velocity fields was quite encouraging. The comparisons were performed at several different times and the wind towers were several hundred meters apart, but the discrepancies between theory and experiment were almost all below twenty percent of the measured values in both magnitude and direction.

Perhaps the most interesting application, however, is a study of the 1991 Oakland Hills fire by Trelles and Pagni [Trelles and Pagni, 1997]. This fire destroyed over two thousand buildings and affected an area of 600 hectares. The initial fire spread was strongly influenced by the dry 10 m/s ambient winds. However, between 11:45 AM and 12:00 noon the observed rate of spread of the fire slowed dramatically. Trelles and Pagni used the model described above to estimate the relative importance of the fire induced and ambient winds. They used estimates of the ambient wind field and the energy release rates associated with single and multiple unit dwellings together with the observed burning patterns at the two times in question. At 11:45 AM they assumed that the 38 observed fires each had a 50 MW heat release rate. The fire induced wind fields, shown in Fig. 3, are a small perturbation on the ambient winds. However, by noon 259 fires were burning at rates estimated to be between 50 MW and 330 MW each. The combined effect of all these fires generated winds up to 13 m/s in places. The computed flow patterns are shown in Fig. 4. These velocities are comparable to those in the ambient wind. Moreover, they are primarily directed towards the most intensely burning regions of the fire. Thus, they impede the spread of the fire on the downwind side of the burning region. This statement is valid whether the spread mechanism is convective and radiative heat transfer from the flames or (as was widely observed) spotting by burning leaves and shingles carried aloft by the winds.

Comparison of this model with large scale field measurements and observations has yielded encouraging results. However, it is important that the model be tested against laboratory experiments, where sources of error can be more precisely defined. Gore and his collaborators have performed a series of experiments and analyses along these lines [Gore et al., 1996], [Zhou and Gore, 1998]. In their most detailed experiments, measurements were made of the vorticity and heat release rate distributions in a 7.1 cm natural gas diffusion burner designed to mimic

the hydrodynamic properties of a small pool fire. The vorticity was obtained from particle imaging velocimetry (PIV) measurements of the velocity field. Time averages of the velocity were then differenced to obtain the vorticity. The sources of the expansion field were obtained by relating them to the local mixture fraction field [Baum, et al., 1990]. The mixture fraction was determined from measurements of the major species concentrations. Figure 5 shows a comparison between PIV measurements of the vertical velocity component and the calculated velocities using the measured sources. Zhou and Gore note, in describing their closely related Fig. 4 [Zhou and Gore, 1998]:

> "The agreement between the predictions and the measurement is excellent. The predictions are not only close to the data in absolute value, but also catch the saddle shape of the radial distribution of axial velocities at locations close to the burner surface. This agreement supports the present method of estimating the source term."

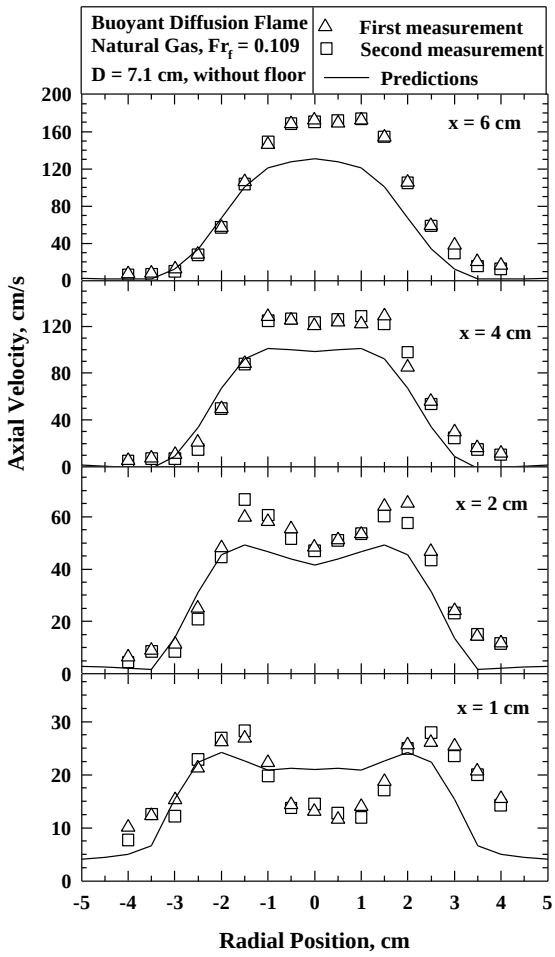

FIGURE 5: COMPARISON OF VERTICAL COMPONENT OF VELOCITY WITH PREDICTIONS BASED ON MEASURED SOURCE TERMS (COURTESY PROF. J. GORE)

WIND BLOWN PLUMES

There is considerable interest in the environmental consequeces of large fires, since the transport of combustion products by a wind-blown fire plume can distribute potentially hazardous materials over a large area. Pools of burning oil and other petroleum products are of particular concern due to the vast flow of these materials through the global economy and because of the fragility of the environment in many regions where oil is extracted, transported, or stored. Buoyant wind-blown plumes have been studied since the 1960's, and an extensive literature has been develped. Summaries of recent work have been given by Turner [Turner, 1985] and Wilson [Wilson, 1993]. Virtually all the models described in these reviews are integral models, where the profiles of physical quantities in cross-sectional planes perpendicular to the wind are assumed, together with simple laws relating plume entrainment to macroscopic features used to describe its evolution. Many of the models in use for air quality assessment simply use Gaussian profiles of pollutant density. Unfortunately, the plume structures actually observed are too complex to be described in terms of a few simple parameters.

Most of the assumptions required by integral models can be removed by taking advantage of the enormous advances in computational fluid dynamics that have occurred since these models were developed. This is especially true if it is assumed that the component of the fluid velocity in the direction of the ambient wind is literally the wind speed. The neglect of streamwise perturbations to the ambient wind is an old idea in aerodynamics, where it has been used to study aircraft wakes since the 1930's [Batchelor, 1967]. Once this approximation is made the plume can be studied as a two-dimensional time dependent entity. The large scale structure of the plume can then be determined in detail at moderate computational cost. The small-scale "sub-grid" mixing and dissipation is represented with a constant eddy viscosity. This permits the mathematical structure of the Navier-Stokes equations to be retained. The effective Reynolds number, defined by the buoyancy induced velocity, plume height, and eddy viscosity, is chosen to be well above 10^4. This permits at least two orders of mag-

nitude of dynamically active length scales in all coordinate directions to be simulated. Thus, the model described here is a simplified form of large eddy simulation.

The plume is described in terms of steady-state convective transport by a uniform ambient wind of heated gases and particulate matter introduced into a stably stratified atmosphere by a continuously burning fire [Baum, et al., 1994], [McGrattan et al., 1996]. Since the firebed itself is not the object under study, only the overall heat release rate and the fraction of the fuel converted to particulate matter need be specified. The simulation begins several fire diameters downwind of the fire, where the plume is characterized by relatively small temperature perturbations, and minimal radiation effects. In this region the plume gases ascend to an altitude of neutral buoyancy, and then gradually disperse. The trajectory of the plume is governed by the ambient wind, the atmospheric stratification and the buoyancy induced convection. It is assumed that the ambient temperature profile as a function of height is available. The model has been extended to allow for multiple interacting plumes [Trelles et al., 1999a] and the presence of a wind shear [Trelles et al., 1999b]. However, only the basic form of the model will be discussed in detail here.

Assuming that the perturbations to the background temperature $T_0(z)$ and pressure $P_0(z)$ are small beyond a few diameters downwind of the firebed, the expansion component of the velocity field can be ignored and the equations describing the steady-state plume reduce to the Boussinesq approximation. The uniform ambient wind speed U is taken to be constant. For mathematical consistency, U is much larger than the buoyancy induced crosswind velocity components, and the rates of change of physical quantities in the windward direction are much slower than those in the crosswind plane. These assumptions are quite realistic several flame lengths downwind of the firebed. Since U does not change, there is no need for a windward component of the momentum equations. The details of the firebed are not being simulated, so the only information about the fire required is the overall convective heat release rate Q_O and the particulate mass flux. The initial temperature distribution in the plume cross section is assumed to be Gaussian and satisfy the following integral

$$\int_{-\infty}^{\infty}\int_{0}^{\infty} \rho_0 c_p U \tilde{T}\, dz\, dy = Q_O \tag{29}$$

The quantity $\tilde{T}$ is the fire induced temperature perturbation. The particulate matter (or any non-reacting combustion product) is tracked through the use of Lagrangian particles which are advected with the overall flow. The initial particulate distribution mimics the initial temperature distribution. If either more detailed experimental data or the results of a local simulation of the fire bed dynamics is available, then these could be used in lieu of the Gaussian profile.

The equations of motion are made non-dimensional so as to maximize the amount of information which can be extracted from each run. First, the windward spatial coordinate is replaced by a temporal coordinate

$$t^* = \frac{V}{UL}\, x \tag{30}$$

where the plume height L is given in terms of the potential temperature of the undisturbed atmosphere $\Theta(z)$.

$$L = \left(\frac{Q_O}{C_p T_0 \rho_0 U \Theta'} \right)_{z=0}^{1/3} \quad ; \quad \Theta'(z) = \frac{1}{\Theta}\frac{d\Theta}{dz} \tag{31}$$

The potential temperature is related to the actual temperature through the relation

$$P_0^{-\kappa}(z)\, T_0(z) = P_0(0)^{-\kappa}\, \Theta(z) \tag{32}$$

where $\kappa = R/C_p$ and R is the gas constant for dry air. The characteristic velocity of the fluid is given by

$$V = \left(\frac{Q_O g}{C_p T_0 \rho_0 U L} \right)_{z=0}^{\frac{1}{2}} \tag{33}$$

The characteristic length L and velocity V scale the crosswind spatial coordinates $(y, z) = L(y^*, z^*)$ and velocities $(v, w) = V(v^*, w^*)$. The quantity $\Theta'(z)$ is scaled by its value at the ground. The temperature perturbation $\tilde{T}$ is made nondimensional by the expression

$$\tilde{T} = \frac{Q_O}{C_p \rho_0 U L^2} T^* \tag{34}$$

Finally, the turbulent Reynolds and Prandtl numbers are defined

$$\mathrm{Re} = \frac{\rho_0 V L}{\mu} \quad ; \quad \mathrm{Pr} = \frac{\mu C_p}{k} \tag{35}$$

The viscosity and thermal conductivity are to be regarded as "eddy" coefficients whose primary role is to provide sinks of kinetic and thermal energy that are actually the result of sub-grid scale dissipative processes. In practice, they are used to set the dynamic range of length scales employed in the simulation, which is typically five to fifteen meters. This range is needed to capture the large-scale fire-induced eddy motions. This requirement, together with the knowledge that the dissipative effects operate at a scale $\mathrm{Re}^{-\frac{1}{2}}$ times smaller than the overall geometric scale (the stabilization height of the plume for this

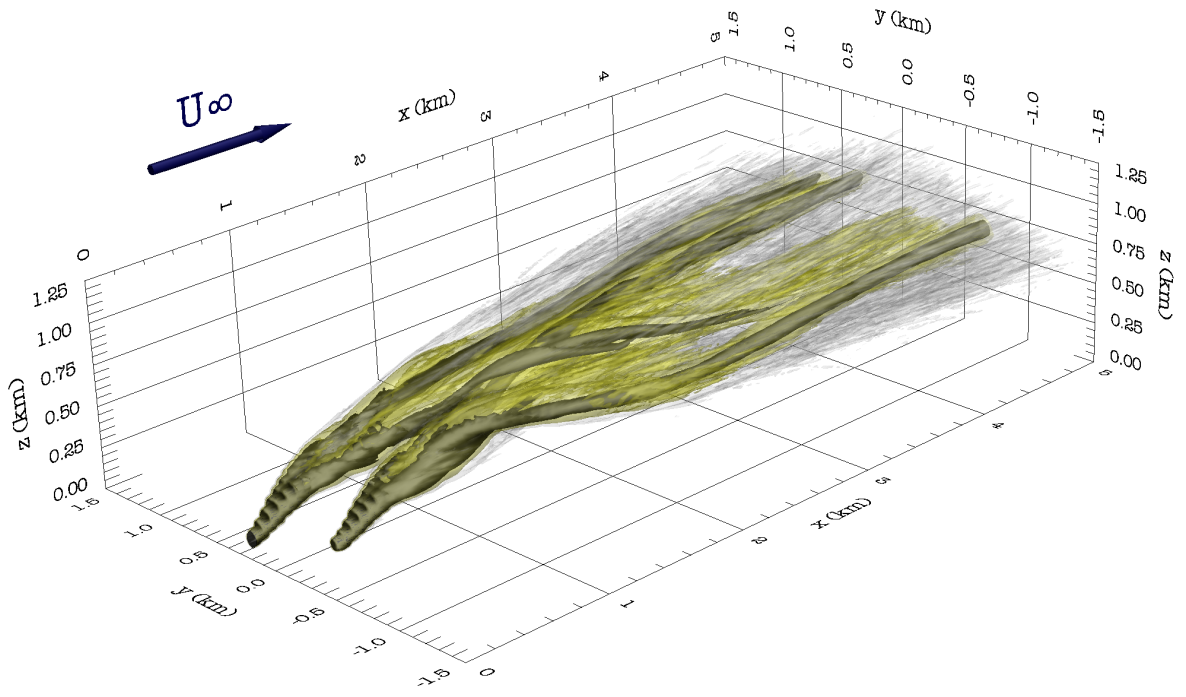

FIGURE 6: TWO INTERACTING 500 MW FIRE PLUMES GENERATED BY OFFSET FIRES 500 M APART. [Trelles et al., 1999a]

problem), translates into Reynolds numbers of the order 10^4. Thermal conductivity is treated in a similar manner to viscosity; thus the Prandtl number remains of order unity.

The dimensionless form of the model equations is remarkably simple

$$\frac{\partial v^*}{\partial y^*} + \frac{\partial w^*}{\partial z^*} = 0 \tag{36}$$

$$\frac{D^* v^*}{D^* t^*} + \frac{\partial p^*}{\partial y^*} = \frac{1}{\mathrm{Re}} \left(\frac{\partial^2 v^*}{\partial {y^*}^2} + \frac{\partial^2 v^*}{\partial {z^*}^2} \right) \tag{37}$$

$$\frac{D^* w^*}{D^* t^*} + \frac{\partial p^*}{\partial z^*} - T^* = \frac{1}{\mathrm{Re}} \left(\frac{\partial^2 w^*}{\partial {y^*}^2} + \frac{\partial^2 w^*}{\partial {z^*}^2} \right) \tag{38}$$

$$\frac{D^* T^*}{D^* t^*} + \Theta^*(z)' \, w^* = \frac{1}{\mathrm{Re}\ \mathrm{Pr}} \left(\frac{\partial^2 T^*}{\partial {y^*}^2} + \frac{\partial^2 T^*}{\partial {z^*}^2} \right) \tag{39}$$

subject to the initial condition

$$\int \int T^*(y^*, z^*)\, dy^*\, dz^* = 1 \tag{40}$$

The crosswind velocity components v^* and w^* are assumed to be zero initially, although this assumption can be relaxed if more detailed information is available. No-flux, free-slip boundary conditions are prescribed at the ground, consistent with the assumed uniformity of the prevailing wind and the resolution limits of the calculation. At the outer and upper edges of the computational domain, the perturbation temperature, perturbation pressure, and windward component of vorticity are set to zero.

Figure 6 shows the results of a sample two plume simulation. The plume is visualized by interpolating the particle locations onto the computational grid, and plotting the isosurface on which the particulate density is a chosen value. Two large counter-rotating vortices are associated with each plume. These vortices are responsible for much of the entrainment, mixing and cooling the combustion gases. These vortices are readily observed in actual large-scale experiments; see Fig. 3 of [McGrattan et al., 1996]. The complexity of even a single plume structure is clearly nothing like that assumed in Gaussian plume models. The computational cost of this simulation is quite modest. A 512 cell (horizontal) by 128 cell (vertical) grid using 15,000 Lagrangian elements to represent the smoke particulate matter re-

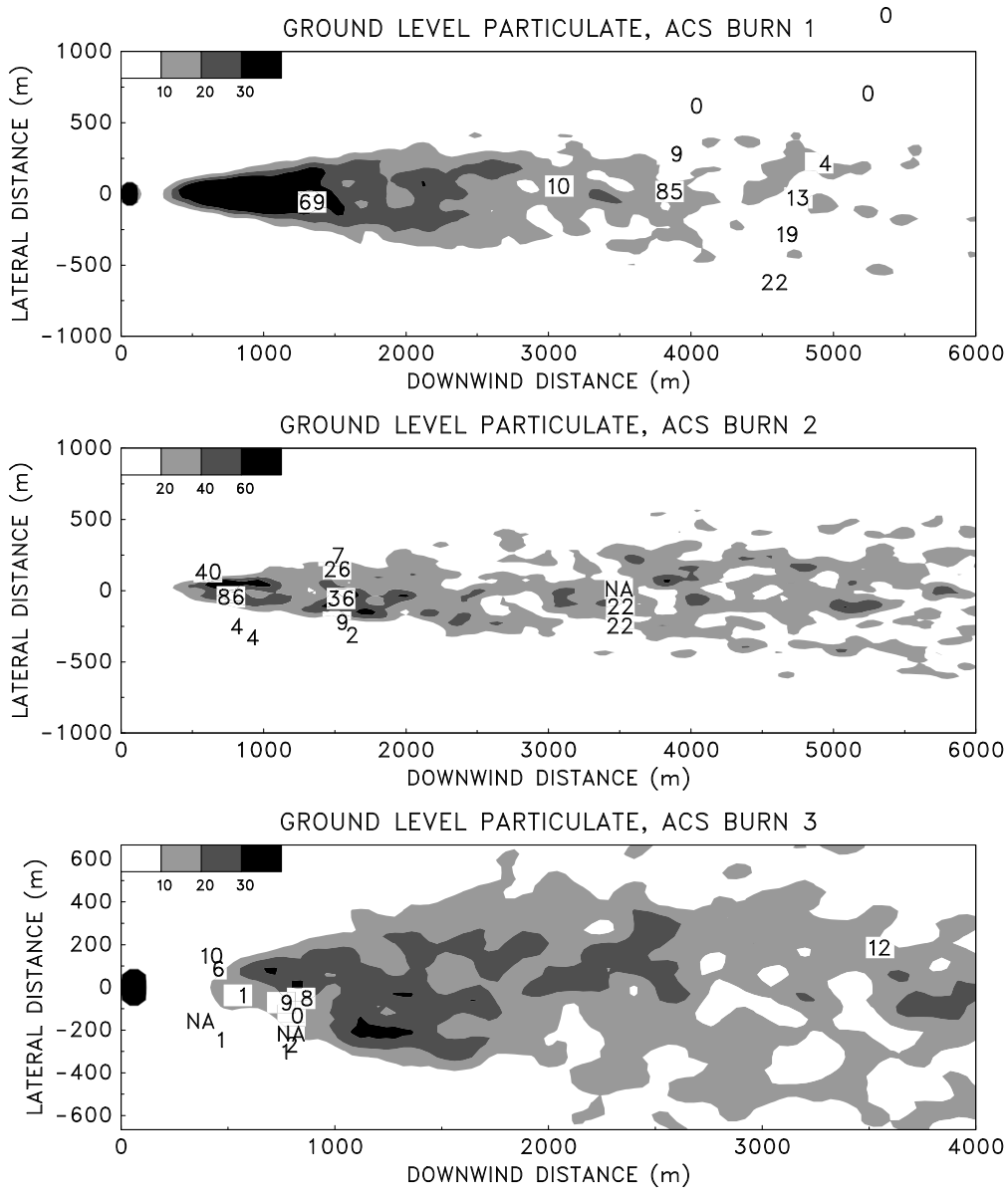

FIGURE 7: PREDICTED GROUND LEVEL PARTICULATE CONCENTRATIONS FROM THE MODEL (SHADED CONTOURS) SHOWN WITH TIME AVERAGED MEASUREMENTS FOR THREE ALASKA CLEAN SEAS EMULSION BURN EXPERIMENTS, SEPT. 1994. [McGrattan et al., 1996]

quires less than 5 minutes on a current generation personal computer to advance the approximately 350 time steps needed to complete the calculation. In fact, over one thousand two plume simulations were performed to explore the large parameter space defined by the multiple plume generalization of this model. All the simulations were performed in the course of a few weeks. Other examples can be found in [Trelles et al., 1999a].

In these simulations, the particles do *not* simply follow the large scale velocity field. The background atmospheric motion plays an equally critical role in determining how rapidly the combustion products disperse. Atmospheric turbulence affects mixing on a wide range of scales, extending to scales which are smaller than the resolution of the calculations performed here. The "eddy" viscosity and thermal conductivity attempt to account for this sub-grid turbulence, but do not account for larger scale, background atmospheric motion. For the present purposes, this motion may be expressed in terms

of variations of the prevailing wind over time scales of minutes to hours. These deviations can be measured, and are introduced into the model through random perturbations to the trajectories of the Lagrangian particles which represent the particulate matter. Thus, the motion of each particle is governed by the fire-induced velocity field found by solving the conservation equations above, plus a perturbation velocity field $(0, v', w')$ which represents the random temporal and spatial variations of the ambient wind. Details of the computation of the random velocity field and a description of the numerical methods employed in the simulation can be found in [McGrattan et al., 1996].

The smoke dispersion predicted by this model has been tested in a variety of large scale field experiments. In early September 1994, Alaska Clean Seas conducted at their Fire Training Ground in Prudhoe Bay, Alaska, three mesoscale burns to determine the feasibility of burning emulsified oil. Each burn consisted of burning an oil mixture within the confines of a fire-resistant circular boom which floated in a pit filled with water. The boom diameter was roughly 9 m, and the rectangular pit was roughly 20 m by 30 m. The first and third burns consumed emulsions of salt water and 17.4% evaporated Alaskan North Slope (ANS) crude. Emulsion breakers were applied to these mixtures. The second burn consumed fresh ANS crude. Heat release rates for the three burns were estimated to be 55, 186 and 98 MW, respectively. The mass flux of particulate was based on a smoke yield for ANS crude of 11.6%.

Figure 7 summarizes the results of the experiments, showing the model prediction of ground level particulate concentration versus the actual measurements made in the field. The field measurements were averaged over the time of the burn. Except for a few stray points, the agreement between the time-averaged model predictions and field measurements is quite good, showing particulate concentrations ranging from 0 to 80 μg m^{-3} along the narrow path over which the plume is lofted. In addition to ground level instruments, a small airplane was hired to fly in the vicinity of the plume and record plume positions at various times, as well as to photograph the burn site and the plume. According to flight track data, the plume from the first burn rose to a height of about 550 m and the plume from the second burn rose to about 400 m. These measurements are in very good agreement with model predictions, based on atmospheric profiles obtained with a helium blimp and a helicopter. In fact, the model predictions were considered accurate enough to use as a planning tool for the siting of the ground based instruments used to record the data shown in Figure 7.

DISCUSSION

The models discussed above represent two limiting cases of large fire scenarios. The kinematic model as applied to the study of mass fires is a case where the overall fire encompasses the entire domain of interest. Here, the details of the distribution of individual fires are all important, while the dynamics of the interaction of the fires with the atmosphere is ignored. If the individual fires are intense enough and persist for a relatively long period of time (tens of minutes, say), then the near ground winds will be dominated by the fire induced flow, and the model is internally consistent. The wind blown plume model, on the other hand, addresses a scenario where the actual combustion zone of the fire is very much smaller than the spatial domain affected by the dispersal of combustion products. Here, the nature of the interaction of the plume with the atmosphere and with other plumes is critical.

In the first case the largest length scale is determined by the geometry of the fire bed, while the individual fire scale $D^\star$ controls the local fire dynamics. In the latter scenario, the interaction of the plume with the atmosphere sets the largest scale L, while the fire bed is typically of negligible dimensions. Any plume interactions typically occur on the L scale. Clearly, each of these limiting cases represents a considerable idealization of any large fire scenario. Atmospheric winds usually cannot be ignored even in large urban fires. The immediate vicinity of the firebed associated with oil spill fires usually is so heavily smoke laden that the absorption of thermal radiation (and hence an absorption length scale) is a significant factor in determining plume dynamics. The geography associated with the natural and built environment is typically a major factor in most large fires. All these imply more length scales, and hence more dimensionless parameters whose influence must be studied, if the dynamics of large fires is to be understood.

REFERENCES

[Batchelor, 1967] Batchelor, G.K., 1967, *An Introduction to Fluid Dymanics*, Cambridge University Press, Cambridge, pp. 580-593.

[Baum, et al., 1990] Baum, H.R., Rehm, R.G., and Gore, J.P., "Transient combustion in a turbulent eddy", *Twenty-Third Symposium (International) on Combustion*, The Combustion Institute, Pittsburgh, pp. 715-722.

[Baum and McCaffrey, 1988] Baum, H.R. and McCaffrey, B.J., 1988, "Fire induced flow field - theory and experiment", *Fire Safety Science - Proceedings of the Second International Symposium*, Hemisphere, New York, pp. 129-148.

[Baum, et al., 1994] Baum, H.R., McGrattan, K.B., and Rehm, R.G., 1994, "Simulation of smoke plumes from large pool fires", *Twenty-Fifth Symposium (International) on Combustion*, The Combustion Institute, Pittsburgh, pp. 1463-1469.

[Goldstein, 1960] Goldstein, S., 1960, *Lectures on Fluid Mechanics*, Interscience, New York, pp. 23-24.

[Gore et al., 1996] Zhou, X.C., Gore, J.P., and Baum, H.R., 1996, "Measurements and predictions of air entrainment rates of pool fires", *Twenty-Sixth Symposium (International) on Combustion*, The Combustion Institute, Pittsburgh, pp. 1453-1459.

[Zhou and Gore, 1998] Zhou, X.C. and Gore, J.P., 1998, "Experimental estimation of thermal expansion and vorticity distribution in a buoyant diffusion flame", *Twenty-Seventh Symposium (International) on Combustion*, The Combustion Institute, Pittsburgh, pp. 2767-2773.

[McCaffrey, 1983] McCaffrey, B.J., 1983, "Momentum implications for buoyant diffusion flames", *Combustion and Flame*, Vol. 52, pp. pp. 149-167.

[McGrattan et al., 1996] McGrattan, K.B., Baum, H.R., and Rehm, R.G., 1996, *Atmospheric Environment*, Vol. 30, pp. 4125-4136.

[Mell et al., 1996] Mell, W.E., McGrattan, K.B., and Baum, H.R., 1996, "Numerical simulation of combustion in fire plumes", *Twenty-Sixth Symposium (International) on Combustion*, The Combustion Institute, Pittsburgh, pp. 1523-1530.

[Quintiere, 1990] Quintiere, J.G., 1990,"Canadian mass fire experiment", National Institute of Standards and Technology Report NISTIR 4444.

[Quintiere, 1993] Quintiere, J.G., 1993, "Canadian mass fire experiment", emphJ. Fire Protection Engineering, Vol. 5, pp. 67-78.

[Rehm and Baum, 1978] Rehm, R.G. and Baum, H.R., 1978, "The equations of motion for thermally driven, buoyant flows", *J. Research of Nat. Bur. Standards*, Vol. 83, pp. 297-308.

[Taylor, 1958] Taylor, G.I., 1958, "Flow induced by jets", *J. Aerospace Sciences*, Vol. 25, pp. 464-465.

[Trelles and Pagni, 1997] Trelles, J. and Pagni, P.J., 1997, "Fire-induced winds in the 20 October 1991 Oakland Hills fire", *Fire Safety Science - Proceedings of the Fifth International Symposium*, Y. Hasemi, Ed., International Association for Fire Safety Science, pp. 911-922.

[Trelles et al., 1999a] Trelles, J., McGrattan, K.B., and Baum, H.R., 1999a, *AIAA J.*, Vol. 37, pp. 1588-1601.

[Trelles et al., 1999b] Trelles, J., McGrattan, K.B., and Baum, H.R., 1999b, *Combustion Theory and Modeling*, Vol. 3, pp. 323-341.

[Turner, 1985] Turner, J.S., 1985, "Proposed pragmatic methods for estimating plume rise and plume penetration through atmospheric layers", *Atmospheric Environment*, Vol. 19, pp. 1215-1218.

[Wilson, 1993] Wilson, R.B., 1993, "Review of development and application of CRSTER and MPTER models", *Atmospheric Environment*, Vol. 27B, pp. 41-57.